Synthetic “smart-gel” based approach toward “electronics-free” artificial pancreas

Akira Matsumoto[1,2], Miyako Tanaka[3], Hiroko Matsumoto[1], Kozue Ochi[3], Yuki Moro-oka[1], Hirohito Kuwata[3,4], Hironori Yamada[1], Ibuki Shirakawa[5], Taiki Miyazawa[1], Hitoshi Ishii[4], Kazunori Kataoka[6,7], Yoshihiro Ogawa[8-10], Yuji Miyahara[1], Takayoshi Suganami[3]

[1]Institute of Biomaterials and Bioengineering, Tokyo Medical and Dental University, Tokyo, Japan.
[2]Kanagawa Institute of Industrial Science and Technology (KISTEC-KAST), Kawasaki, Japan.
[3]Department of Molecular Medicine and Metabolism, Research Institute of Environmental Medicine, Nagoya University, Nagoya, Japan.
[4]Department of Diabetology, Nara Medical University, Nara, Japan.
[5]Department of Organ Network and Metabolism, Graduate School of Medical and Dental Sciences, Tokyo Medical and Dental University, Tokyo, Japan.
[6]Innovation Center of NanoMedicine, Institute of Industrial Promotion – KAWASAKI, Kawasaki, Japan.
[7]Policy Alternatives Research Institute, The University of Tokyo, Tokyo, Japan.
[8]Department of Molecular Endocrinology and Metabolism, Graduate School of Medical and Dental Sciences, Tokyo Medical and Dental University, Tokyo, Japan.
[9]Department of Medicine and Bioregulatory Science, Graduate School of Medical Sciences, Kyushu University, Fukuoka, Japan.
[10]Japan Agency for Medical Research and Development, CREST, Tokyo, Japan.

Background and Aims: Although prior studies attempted to create “electronics-free” insulin delivery systems using glucose oxidase and sugar-binding lectins as a glucose-sensing mechanism, no successful clinical translation has hitherto been made. Indeed, these protein-based materials are intolerant of long-term use and storage due to their denaturing and/or cytotoxic properties.

Method: Here we provide a solution, that is, protein-free and totally synthetic material-based approach. Capitalizing on sugar-responsive property of boronic acid, we have established a synthetic polymer gel-based insulin delivery device confined within a single catheter, which exhibits an artificial pancreas-like function *in vivo*.

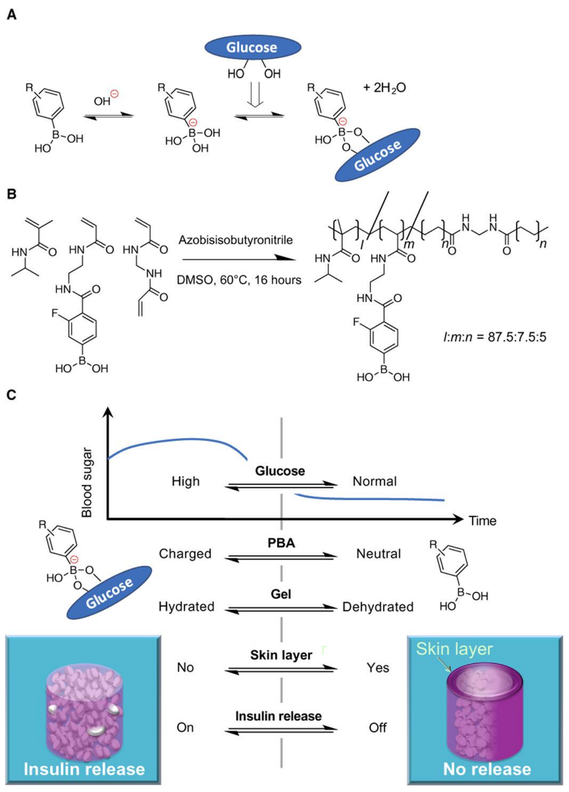

Fig. 1 Structure and principle of the boronate gel–based insulin delivery system.(**A**) Glucose-dependent equilibria of PBA derivatives. (**B**) Chemical structure of glucose-responsive gel. Monomers and their polymerized (cross-linked) chemical structures are shown with their optimized molar fraction (*l*:*m*:*n* = 87.5:7.5:5) to yield the glucose sensitivity under physiological conditions (pH 7.4 and 37° C) accompanied by a threshold concentration of glucose at normoglycemic (100 mg/dl) (above which the gel delivers insulin). DMSO, dimethyl sulfoxide. (**C**) Schematic illustration of “pancreas-like” self-regulated insulin delivery function of the gel.

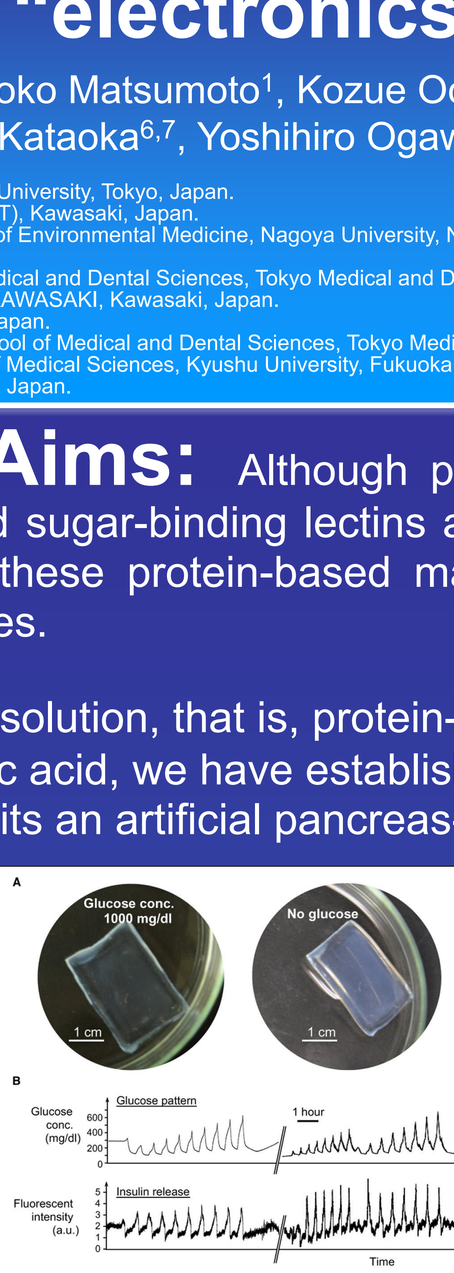

Fig. 2 Characterization of the glucose-responsive gel in vitro.(**A**) Images of a smart gel formed in a macroscopic slab shape equilibrated under hyperglycemic (1000 mg/dl) (left) and no-glucose (right) conditions. (**B**) Release experiment. Top: Temporal patterns of glucose fluctuation challenged through a HPLC setup under physiological conditions (pH 7.4; 37° C; 155 mM NaCl). Bottom: Time course change in fluorescence intensity of fluorescein isothiocyanate (FITC)–labeled bovine insulin released from the gel. The break in the *x* axis indicates an overnight interval between two experiments during which the gel was kept under constant flow (1 ml/min) of phosphate-buffered saline (PBS) containing glucose (100 mg/dl). a.u., arbitrary units.

Totally synthetic Glucose-responsive gel

✓A glucose-dependent shift in the equilibria of PBA (between uncharged and anionically charged; Fig. 1A), when integrated with optimally amphiphilic acrylamide gel backbone (Fig. 1B), could induce a reversible, glucose-dependent change in hydration of the gel.

✓ The resultant abrupt and rapid change in hydration, under optimized conditions, led to the formation of a gel surface–emerging, microscopically dehydrated layer, so-called “skin layer”, providing a mode that is able to effectively switch the release (diffusion) of the gel-loaded insulin (Fig. 1C).

✓ The chemical structure of the gel could be further optimized so that it undergoes the above-mentioned performance under physiologically relevant conditions, accompanied by a remarkably “gated” manner in response to the level of normoglycemia.

Matsumoto, A. *et al. Chem. Lett.* 2016, 45(4), 460-462.
Matsumoto, A. *et al. Angew. Chem. Int. Ed.*, 2012, 51, 2124-2128.
Matsumoto, A. *et al. Chem. Commun.*, 2010, 46, 2203-2205.
Matsumoto, A. *et al. Biomacromolecules* 2004, 5, 1038-1045.
Matsumoto, A. *et al. Biomacromolecules* 2003, 4, 1410-1416.
Kataoka, K. *et al. J. Am. Chem. Soc.* 1998, 120, 12694-12695.

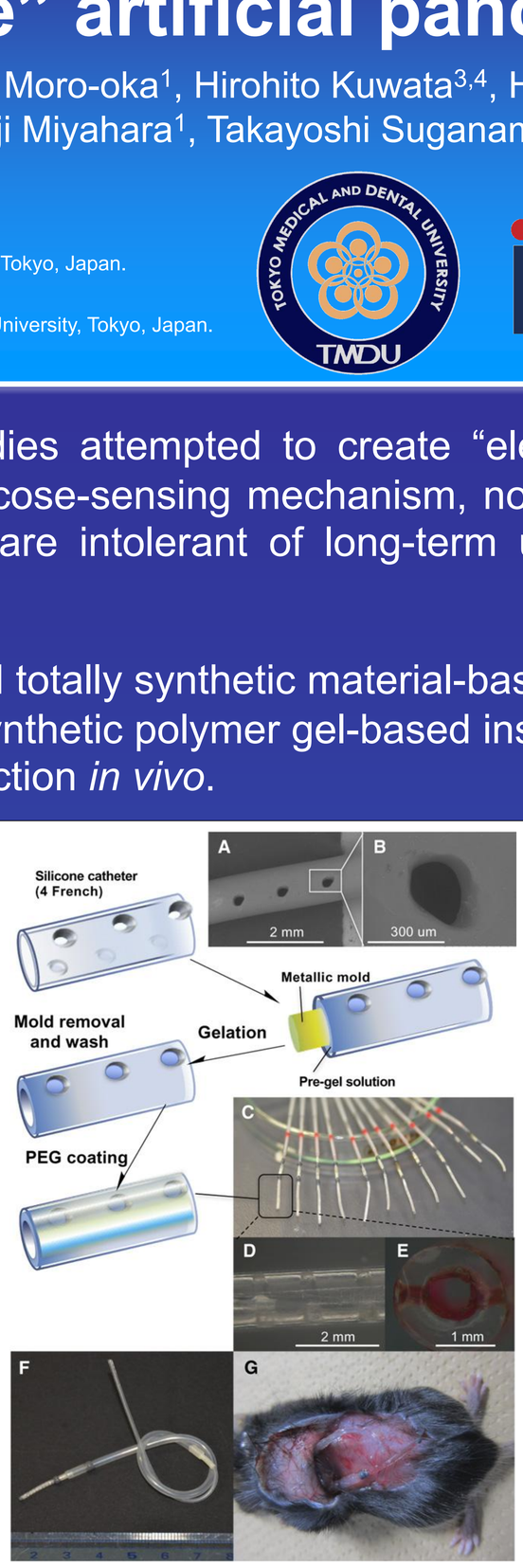

Fig. 3 Fabrication of catheter-combined device.(**A** and **B**) SEM images of 4-French (1.2 mm in diameter) silicone catheter bearing penetrating (perpendicular to the long axis) openings on the wall made by laser irradiation. (**C** to **E**) Overview (C), side view (D), and cross-sectional transmittance images (E) of the gel-modified catheter (the gel was stained by red-colored ink). (**F** and **G**) Overview of the ready-to-use device installed with the upstream (long tail) reservoir filled with insulin and its appearance on subcutaneous implantation. PEG, poly(ethyleneglycol).

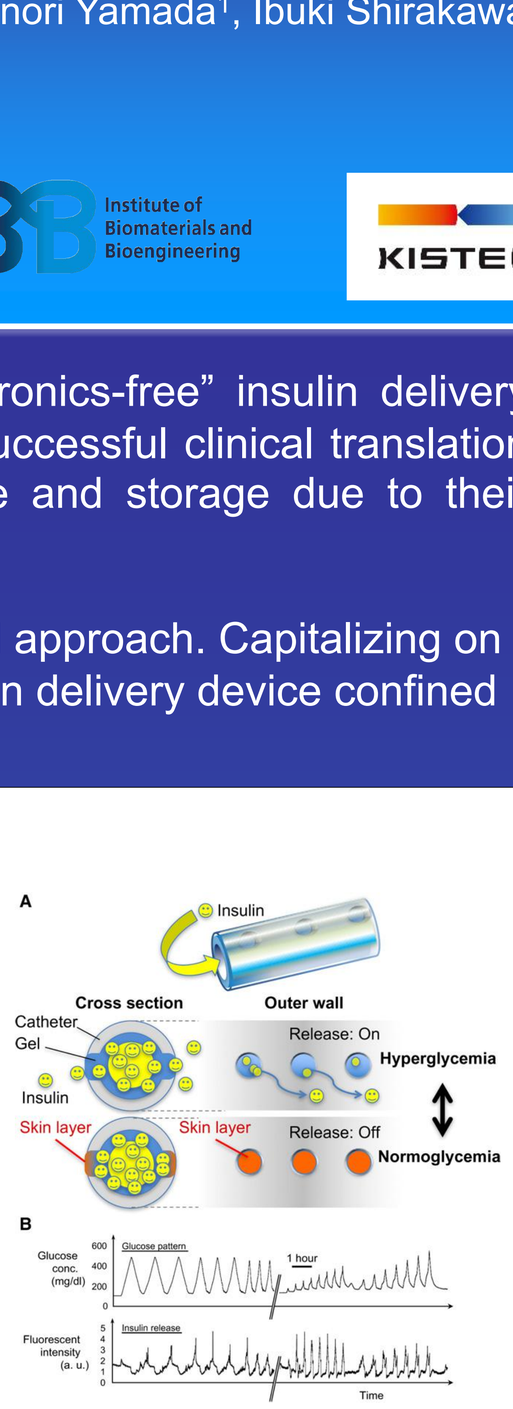

Fig. 4 Working principle and behavior of catheter-combined device.(**A**) Schematic illustration of skin layer–driven glucose-dependent diffusion control of insulin accomplished by the catheter-combined device. (**B**) Release experiment under physiological conditions using a HPLC setup. Top: Temporal patterns of glucose. Bottom: Time course change in fluorescence intensity of FITC-labeled bovine insulin released from the gel. The break in the *x* axis indicates an overnight interval between two experiments during which the device was kept under constant flow (1 ml/min) of PBS containing glucose (100 mg/dl).

Matsumoto, A. *et al*. *Sci. Adv.* 3, eaaq0723(2017)

Results: Subcutaneous implantation of the device in healthy and diabetic mice establishes a closed-loop system composed of “continuous glucose-sensing” and “skin-layer”-regulated insulin release. As a result, the glucose metabolism was controlled in response to the interstitial glucose fluctuation under both insulin-deficient and insulin-resistant conditions with at least three-week durability.

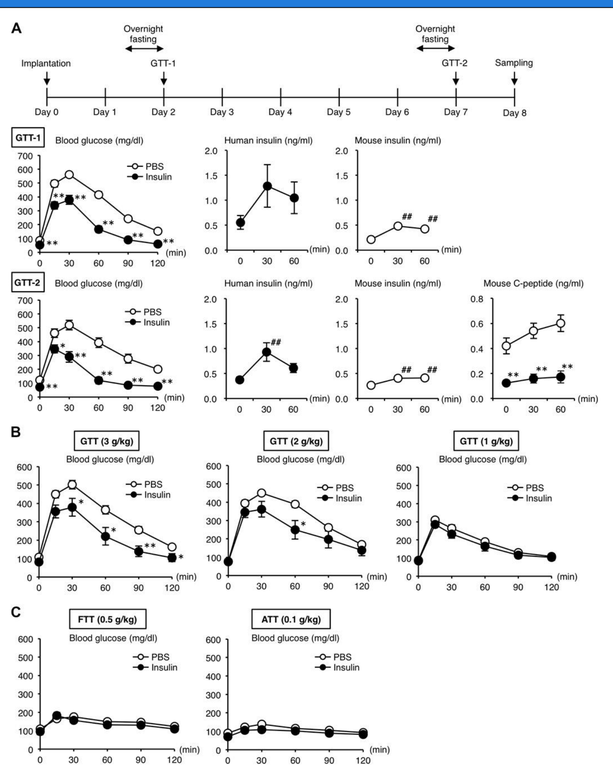

Fig. 5 Evaluation of glucose-responsive insulin release in vivo.(**A**) Protocol of the experimental design using healthy mice. (**B**) Glucose tolerance test (GTT). Glucose (3 g/kg body weight) was injected intraperitoneally 2 and 7 days after the implantation of the devices. $^{**}P < 0.01$ and $^{*}P < 0.05$ versus PBS group. $^{\#\#}P < 0.01$ and $^{\#}P < 0.05$ versus 0 min. $n = 8$ to 12. (B) GTT with different dosage of glucose (1, 2, and 3 g/kg body weight). $^{*}P < 0.05$. $n = 10$. (**C**) The fructose tolerance test (FTT) (fructose, 0.5 g/kg body weight) and the aspartame tolerance test (ATT) (aspartame, 0.1 g/kg body weight). $^{**}P < 0.01$ and $^{*}P < 0.05$. $n = 8$.

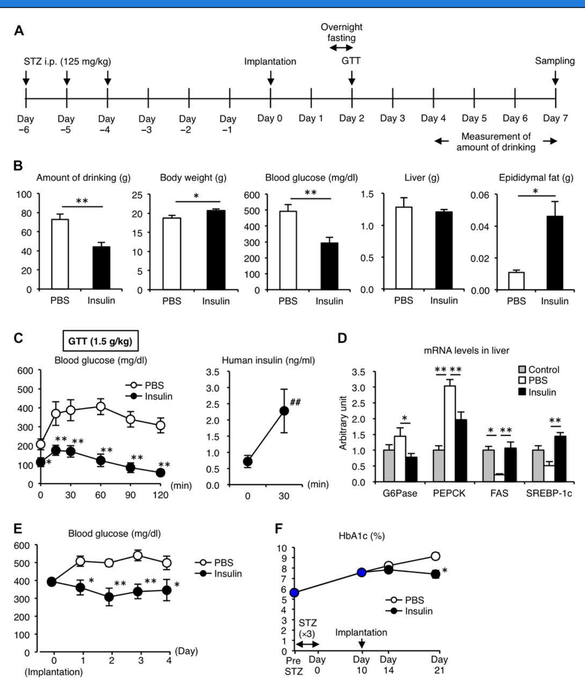

Fig. 6 Therapeutic efficacy for type 1 diabetes in mice.(**A**) Protocol of the experimental design. Type 1 diabetic models were induced by the intraperitoneal (i.p.) injection of STZ (125 mg/kg body weight) for 3 consecutive days. (**B**) Amount of drinking during the last 3 days of the experimental period and body weight, blood glucose concentrations, and tissue weights of the liver and epididymal fat at day 7. (**C**) Blood glucose concentrations and serum human insulin concentrations in the GTT (glucose, 1.5 g/kg body weight). (**D**) mRNA expression of glucose-6-phosphatase (G6Pase), phosphoenolpyruvate carboxykinase (PEPCK), fatty acid synthase (FAS), and sterol regulatory element–binding protein-1c (SREBP-1c) in the liver. $^{**}P < 0.01$ and $^{*}P < 0.05$ versus PBS group. $^{\#\#}P < 0.01$ versus 0 min. $n = 6$ to 12. (**E**) Blood glucose concentrations under ad lib–fed conditions after implantation of the device. $^{*}P < 0.05$. $n = 6$ to 12. (**F**) Time course of HbA1c. Type 1 diabetic mice were implanted with the device containing PBS and human insulin. $^{*}P < 0.05$. $n = 4$.

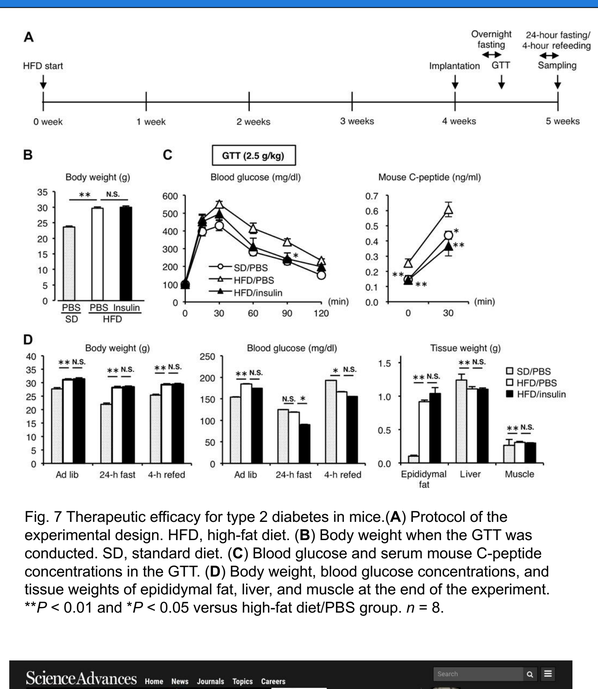

Fig. 7 Therapeutic efficacy for type 2 diabetes in mice.(**A**) Protocol of the experimental design. HFD, high-fat diet. (**B**) Body weight when the GTT was conducted. SD, standard diet. (**C**) Blood glucose and serum mouse C-peptide concentrations in the GTT. (**D**) Body weight, blood glucose concentrations, and tissue weights of epididymal fat, liver, and muscle at the end of the experiment. $^{**}P < 0.01$ and $^{*}P < 0.05$ versus high-fat diet/PBS group. $n = 8$.

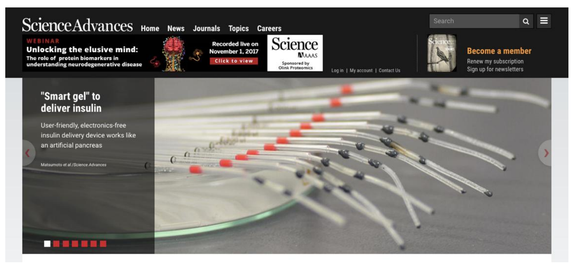

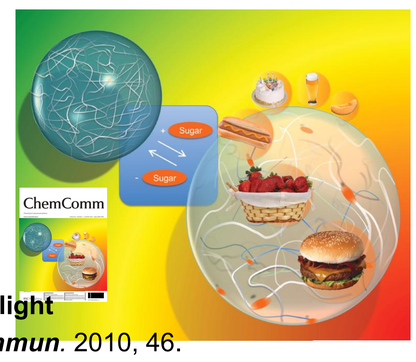

Cover Highlight
Chem. Commun. 2010, 46.

Cover Highlight
Angew. Chem. 2012, 51.

Web highlight: http://advances.sciencemag.org/
Sci. Adv. **3, eaaq0723(2017)**

Summary: Our “smart-gel” technology could offer user-friendly and remarkably economic (disposable) alternative to the current state-of-the-art, thereby facilitating prevalence not only to developing countries, but also to those who otherwise may not be strongly motivated such as the elderly, infants, patients in need of nursing care and even patients averse to electrical and mechanical medical devices.

Acknowledgement: The authors thank Dr. Ryo Miyake (The University of Tokyo, Japan) for technical advice in micro-processing of catheter. This work was supported in part by Grants-in-Aid for Scientific Research from the Ministry of Education, Culture, Sports, Science and Technology of Japan, Japan Science and Technology Agency (JST: START program and COI stream) and Japan Agency for Medical Research and Development (AMED: ACT-M program). This work was also supported by research grants from The Canon Foundation, Secom Science and Technology Foundation, Terumo Foundation for Life Sciences and Arts, the Mochica Memorial Foundation for Medical and Pharmaceutical Research and the Research Center for Biomedical Engineering.